# Vacancy defects and the formation of local haeckelite structures in graphene from tight-binding molecular dynamics

Gun-Do Lee,[1] C. Z. Wang,[3] Euijoon Yoon,[1] Nong-Moon Hwang,[2] and K. M. Ho[3]
[1]*School of Materials Science and Engineering and Inter-university Semiconductor Research Center (ISRC), Seoul National University, Seoul 151-742, Korea*
[2]*National Research Laboratory of Charged Nanoparticles, School of Materials Science and Engineering, Seoul National University, Seoul 151-742, Korea*
[3]*Ames Laboratory and Department of Physics and Astronomy, Iowa State University, Ames, Iowa 50011, USA*
(Received 8 June 2006; revised manuscript received 20 October 2006; published 11 December 2006)

The dynamics of multivacancy defects in a graphene layer is investigated by tight-binding molecular dynamics simulations and by first principles calculation. The simulations show that four single vacancies in the graphene layer first coalesce into two double vacancies, each consisting of a pentagon-heptagon-pentagon (5-8-5) defective structure. While one of the 5-8-5 defects further reconstructs into a 555-777 defect, which is composed of three pentagonal rings and three heptagonal rings, another 5-8-5 defect diffuses toward the reconstructed 555-777 defect. During the 5-8-5 defect diffusion process, three interesting mechanisms, i.e., "dimer diffusion," "chain diffusion," and "single atom diffusion," are observed. Finally, the four single vacancies reconstruct into two adjacent 555-777 defects, which is a local haeckelite structure.

DOI: 10.1103/PhysRevB.74.245411 PACS number(s): 61.72.Ji, 81.05.Uw, 61.80.Az, 71.15.Pd

## I. INTRODUCTION

Vacancy is one of the most common defects in crystalline solids and affects profoundly the physical properties of the solids. Low concentration of vacancy defects present in graphite[1] during defective growth or as part of the thermal equilibrium process. These defects are much more prevalent in electron or ion irradiated materials and are believed to be the predominant defects on irradiated graphite surfaces.[2] Since graphite is commonly used as a substrate in various microscopy techniques,[3] characterization of surface defect in graphite at the atomic scale is an important research drive. Point defects induced by irradiation damage in graphite is also a subject of great scientific and technological interest because of the application of graphite as moderators in thermal nuclear reactors.[4] Furthermore, the emerging field of carbon nanoscience[5] shares a lot of useful information from graphitic systems including defect structure and energetics. Various carbon nanostructures such as carbon nanotube branched junctions[6–8] have been produced through generation and recombination of vacancy defects in single-walled carbon nanotubes.

Vacancy in graphitic systems has attracted considerable experimental and theoretical studies for many years. Various advanced experimental techniques such as scanning tunneling microscope (STM),[2] positron annihilation spectroscopy,[9] and transmission electron microscope[10] have been used to investigate the structure and properties of vacancies in graphite and carbon nanotubes. At the same time, a number of theoretical calculations have also been performed to study the vacancy in graphite.[11–15] However, most of the previous theoretical studies focused only on the structure of single vacancy. Much less is known for the dynamics of the vacancy as well as the structure and dynamics of multivacancies. In order to gain more information about the structures of multivacancies, the dynamical behavior of vacancies, and the effects of vacancies on the structure and stability of the graphene layer, atomistic simulation studies of multivacancies in a graphene layer will be very useful and highly desirable.

Since classical molecular dynamics simulations are not reliable for studying such complex systems as vacancy defects in graphite or carbon nanotube and *ab initio* molecular dynamics is too expensive for long time dynamical simulation of large systems, we chose to perform the quantum molecular dynamics simulation for these systems using the tight-binding molecular dynamics (TBMD) method. Recently, we have modified the environment-dependent tight-binding (TB) carbon potential by Tang *et al.*[16] We have also used this modified TB potential to investigate the structure and energetics of vacancy and adatoms in a graphene layer and carbon nanotube and performed TBMD simulations to study the dynamics of vacancy in a graphene layer. In this paper, TBMD simulation studies of the structure and dynamics of multivacancies in a graphene layer will be reported. In particular, the collective behavior of the vacancies and the diffusion of a double vacancy observed from the TBMD simulations will be discussed in detail.

## II. CALCULATIONAL METHOD

The TBMD simulations are performed using the recently modified environment dependent tight-binding (EDTB) carbon potential. We note that the original EDTB carbon potential by Tang *et al.* is not sufficient to describe the angle dependence of the bonds because the effective interatomic distance is scaled only by the coordination number which is not angular sensitive.[16] In our modified potential, the angle dependence of bonds is taken into account by redefining the

 

coordination number for the repulsive term of the interaction according to the geometric anisotropy of the atoms. Specifically, the coordination number for repulsive interaction in the modified potential is expressed as

$$n_i = n_{oi} K(n_{oi}, \eta_i), \tag{1}$$

where $n_{oi}$ is the coordination number in the original potential[16] and $K(n_{oi}, \eta_i)$ is an anisotropy function where $\eta_i$ is the anisotropy factor which is given by

$$\eta_i = \sqrt{\left(\sum_k (1 - S_{ik}) x_{ik} \tau(r_{ik})\right)^2 + \left(\sum_k (1 - S_{ik}) y_{ik} \tau(r_{ik})\right)^2 + \left(\sum_k (1 - S_{ik}) z_{ik} \tau(r_{ik})\right)^2}, \tag{2}$$

where $S_{ik}$ is the screening function as defined in the original potential,[16] and $x_{ik}$, $y_{ik}$, and $z_{ik}$ are the $x$, $y$, and $z$ coordination of $r_{ik}$, respectively. $\tau(r_{ik})$ is a Fermi-Dirac–type attenuation function expressed as $1/[\exp(\beta(r_{ik}-r_c))+1]$ which gives zero at large distance between $i$th and $k$th atom ($r_{ik} \gg r_c$). The values for $\beta$ and $r_c$ are chosen to be 10.0 and 2.0 Å, respectively. The anisotropy function $K(n_{oi}, \eta_i)$ is expressed in a numerical form and equal to 1 when $\eta_i=0$. This numerical function is determined by fitting to the structures and energies of a number of defects in graphene from first principles calculations. Note that for a perfect crystalline solid $\eta_i$ is zero due to the symmetry and $n_i$ is reduced to the original form of the coordination number, $n_{oi}$. Therefore, the energies of the graphite, diamond, simple cubic, bcc, and fcc bulk structures from the modified potential are the same as that from the original one. The accuracy of the modified EDTB carbon potential for defects in graphene has been well demonstrated in our previous paper,[17] where the potential was successfully applied to the study of double vacancy in a graphene layer.

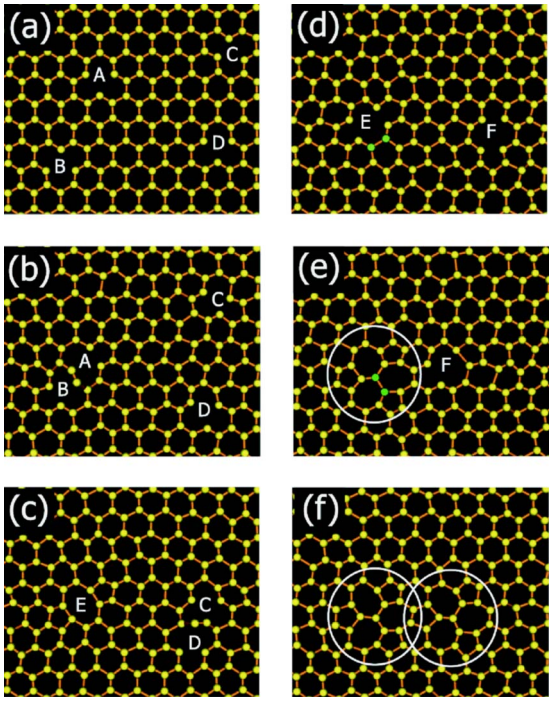


FIG. 1. (Color online) Atomic processes from the TBMD simulations of four vacancy defects in a graphene layer. (a) 0 K (at time $t$=0 ps) [from Fig. 4(a) in Ref. 17]; (b) ~3000 K ($t$=5.5 ps); (c) ~3000 K ($t$=52.6 ps); (d) ~3900 K ($t$=86.8 ps); (e) ~3700 K ($t$=274.4 ps); (f) ~3700 K ($t$=281.6 ps) [from Fig. 4(b) in Ref. 17].

In the present simulation, the unit cell consists of a single graphene layer of 212 carbon atoms and a vacuum region of 13 Å in the direction perpendicular to the graphene layer, and four carbon atoms are removed to create four single vacancies. Periodic boundary conditions are used in all three dimensions. We have also performed first-principles calculations with the same unit cell to verify some key diffusion barriers for the vacancies suggested from the TBMD simulation. First principles total energy calculations are carried out employing the plane wave basis Vienna *ab initio* simulation pack (VASP) code.[18–20] Vanderbilt pseudopotentials[21] are used in this calculation. In the first principles calculation, the basis set contains plane waves up to an energy cutoff of 400 eV and 13 **k** points are selected in the two-dimensional irreducible Brillouin zone. When structural relaxations are performed in the first-principles or TB calculations, the structure is relaxed until the force on each atom is less than 0.02 eV/Å (except for those atoms whose coordinates are intentionally held during the relaxation).

## III. RESULT AND DISCUSSION

The TBMD simulation begins with four separated single vacancies in a graphene layer which are fully relaxed by TB calculation by using the steepest descent method. In order to investigate the structural transformation induced by the vacancies, we perform TBMD simulation at high temperature starting from the relaxed geometry as shown in Fig. 1(a). After a simulation time of 85 ps with a constant temperature of 3000 K, the temperature is increased to about 3800 K to accelerate the dynamics. Some snapshots about the diffusion, coalescence, and reconstruction process of the four single vacancies during the TBMD simulation are shown in Fig. 1 and are discussed below.

In Fig. 1(b), the single vacancy $A$ is found to approach the single vacancy $B$ through a sequence of diffusion while the single vacancies $C$ and $D$ also change their orientations and positions with respect to each other. It has been shown that single vacancy diffusion in a graphene layer is triggered by single atom hopping and the energy barrier for the diffusion has been reported to be 0.94 eV by a first principles local

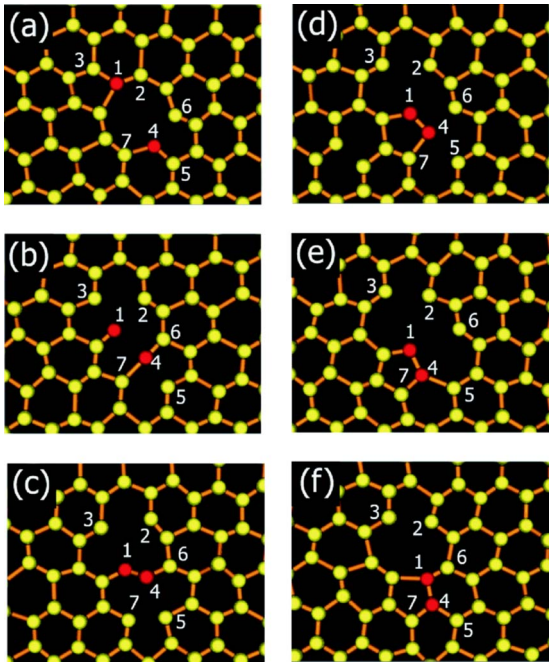


FIG. 2. (Color online) Diffusion of 5-8-5 vacancy by the "dimer diffusion" mechanism. (a) ~3900 K ($\Delta t$=0 ps); (b) ~3800 K ($\Delta t$=0.09 ps); (c) ~4100 K ($\Delta t$=0.20 ps); (d) ~3800 K ($\Delta t$=0.33 ps); (e) ~3900 K ($\Delta t$=0.36 ps); (f) ~3900 K ($\Delta t$=0.47 ps). (a) Snapshot at total simulation time $t$=170.5 ps. $\Delta t$ is the elapsed time relative to the time at (a). Note that carbon atoms in red color play an important role in the "dimer diffusion" mechanism.

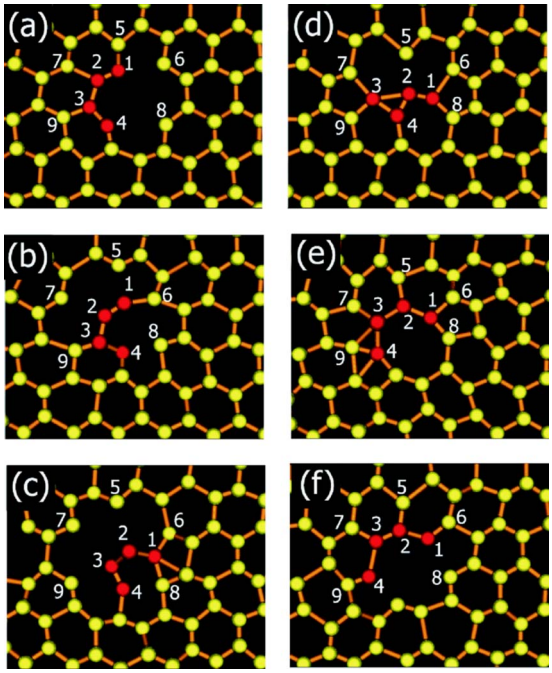


FIG. 3. (Color online) Diffusion of 5-8-5 vacancy by the "chain diffusion" mechanism. (a) ~4000 K ($\Delta t$=0 ps); (b) ~3700 K ($\Delta t$=0.38 ps); (c) ~3900 K ($\Delta t$=0.41 ps); (d) ~3600 K ($\Delta t$=0.48 ps); (e) ~4100 K ($\Delta t$=0.52 ps); (f) ~3700 K ($\Delta t$=0.58 ps). (a) Snapshot at total simulation time $t$=176.9 ps. $\Delta t$ is the elapsed time relative to the time at (a). Note that carbon atoms in red color form a chain and play an important role in the "chain diffusion" mechanism. See text for more details.

density approximation (LDA) calculation.[17] At the simulation time of 6.5 ps, the single vacancies $A$ and $B$ are found to coalesce into a double vacancy $E$ [Fig. 1(c)] by rotation and diffusion of the carbon dimer between two single vacancies. The double vacancy $E$ is a pentagon-octagon-pentagon (5-8-5) defective structure. In Fig. 1(c), the single vacancy $C$ also approaches the single vacancy $D$ through a sequence of single carbon atom diffusion and becomes a neighboring vacancy with $D$. The single vacancies $C$ and $D$ then also coalesce into a 5-8-5 double vacancy $F$ as shown in Fig. 1(d) in a way similar to the formation of the double vacancy $E$ in Fig. 1(c), i.e., through the rotation and diffusion of the dimer between two single vacancies. The detailed process of such double vacancy formation has been reported in our previous paper.[17] At the total simulation time of 128 ps, the double vacancy $E$ is further reconstructed into a defect structure of three pentagons and three heptagons (555-777), as indicated by the white circle in Fig. 1(e), by 90° rotation of the carbon dimer indicated by green color, i.e., by the Stone-Wales transformation.[22] It is very interesting to note that while the double vacancy $E$ is reconstructed into the 555-777 defect, the 5-8-5 vacancy $F$ had diffused to the vicinity of the 555-777 defect as shown in Fig. 1(e). In the diffusion process of the double vacancy $F$, some interesting mechanisms have been observed, which will be discussed in more detail later in this paper. Note that the double vacancy $F$ is also eventually reconstructed into a 555-777 defect in Fig. 1(f) and the formation of two adjacent 555-777 defects, as indicated by two white circles in Fig. 1(f), is observed. It has been suggested by Terrones *et al.* that the 555-777 defect structure is a building block of the hexagonal ($H_{5,6,7}$) haeckelite structure.[23] Thus, through the sequential diffusion and reconstruction, four scattered single vacancies are finally transformed into a local hexagonal ($H_{5,6,7}$) haeckelite structure. The haeckelite structure is interesting because it has been shown that haeckelite tube exhibits an intrinsic metallic behavior, independent of orientation, tube diameter, and chirality. Our present simulation of vacancy defects in graphene layer suggests that hexagonal ($H_{5,6,7}$) haeckelite structures can be produced by heating graphene layers up to a proper high temperature after irradiation.

As we mentioned earlier, diffusion of the 5-8-5 vacancy defect is observed in our TBMD simulation between Figs. 1(d) and 1(e). During this diffusion process, three different diffusion mechanisms, i.e., "dimer diffusion," "chain diffusion," and "single atom diffusion" have been identified.

The "dimer diffusion" mechanism, which is illustrated in Fig. 2, is observed in the initial diffusion process of the 5-8-5 vacancy at the total simulation time of 170.5 ps. As shown in Fig. 2, atom 1 breaks the bonds with atoms 2 and 3 and diffuses toward atom 4, while atom 4 breaks the bond with atom 5 and forms a bond with atom 6 [Fig. 2(b)]. In Fig. 2(c), carbon atoms 1 and 4 form a carbon dimer. At the same time, atom 4 breaks the bond temporarily with atom 7 and the double vacancy is temporarily split into two single vacancies. After formation of the dimer, the two carbon atoms 1 and 4 diffuse together as a unit. Through diffusion and

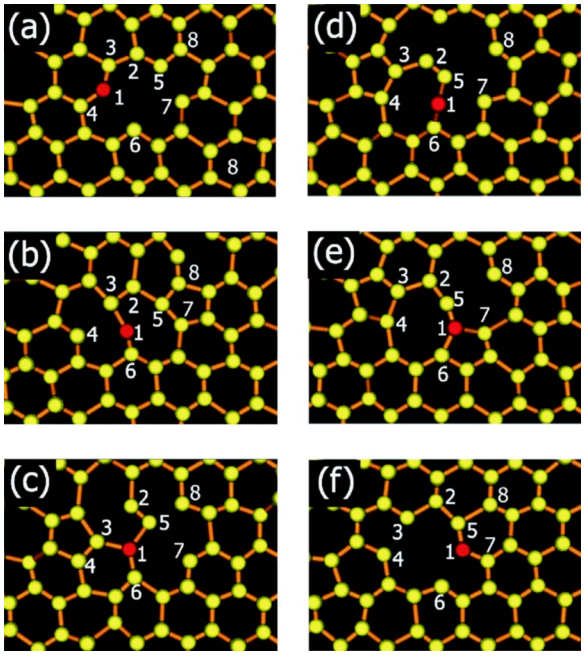


FIG. 4. (Color online) Diffusion of 5-8-5 vacancy by the "single atom diffusion" mechanism. (a) ~3800 K ($\Delta t$=0 ps); (b) ~4100 K ($\Delta t$=0.28 ps); (c) ~3900 K ($\Delta t$=0.44 ps); (d) ~3900 K ($\Delta t$=0.51 ps); (e) ~4100 K ($\Delta t$=0.61 ps); (f) ~3800 K ($\Delta t$=0.69 ps). (a) Snapshot at total simulation time $t$=196.7 ps. $\Delta t$ is the elapsed time relative to the time at (a). Note that the carbon atom in red color plays an important role in the "single atom diffusion" mechanism. See text for more details.

rotation of the dimer [Figs. 2(c)–2(e)] new 5-8-5 vacancy is generated as shown in Fig. 2(f) but the center of the 5-8-5 vacancy has been moved as compared to that in Fig. 2(a). In this mechanism, the pentagon-pentagon (5-5) axis of the 5-8-5 vacancy is found to rotate clockwise by ~60° from Fig. 2(a) to Fig. 2(f). The energy barrier for the "dimer diffusion" mechanism is found to be 7.6 eV by first principles LDA calculation.

Figure 3 illustrates the "chain diffusion" mechanism which is observed at the total simulation time of 176.9 ps. In the early stage of the "chain diffusion," carbon atom 1 breaks the bond with atom 5 and forms a bond with atom 6 while atom 2 breaks the bond with atom 7 as shown in Fig. 3(b). In Fig. 3(c), atom 1 forms a bond with atom 8 and atom 3 breaks the bond with atom 9. Then, atom 3 forms a bond with atom 7 in Fig. 3(d) and atom 4 forms a bond with atom 9 by ~60° clockwise rotation of a carbon dimer (atoms 3 and 4) in Fig. 3(e). Consequently, the diffusion of carbon atoms 1 and 2 [Figs. 2(a)–2(d)] induces the diffusion of carbon atoms 3 and 4 [Figs. 2(d)–2(f)]. Finally, Fig. 3(f) shows that the carbon chain composed by atoms 1–4 has been moved curvilinearly by a clockwise rotation as compared to the same carbon chain in Fig. 3(a). Due to the diffusion of the carbon chain shown in Figs. 3(a)–3(c) and 3(f), the 5-8-5 vacancy diffuses downward and rotates by clockwise rotation of ~60°. The energy barrier for this "chain diffusion" mechanism is found to be 6.6 eV by first principles LDA calculation.

Finally, the "single atom diffusion" mechanism is shown in Fig. 4. In this mechanism, diffusion of the 5-8-5 vacancy

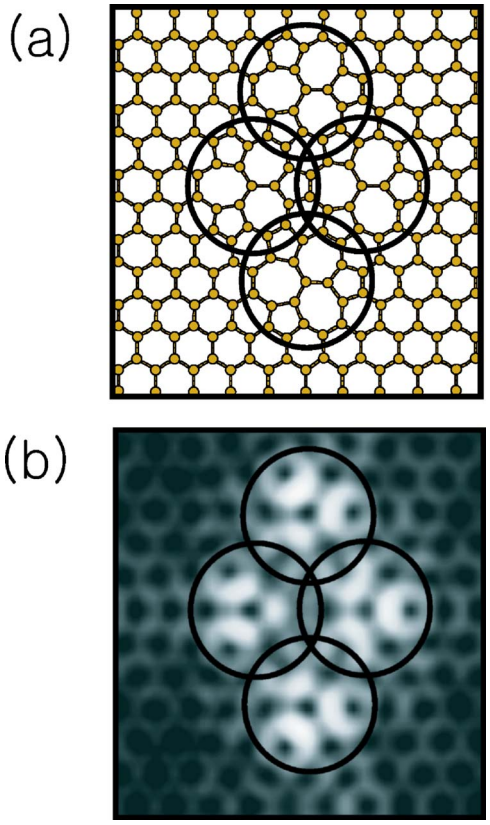


FIG. 5. (Color online) (a) Atomic structure of a graphene layer with four neighboring 555-777 defects and (b) the corresponding simulated STM image of a filled state at $V_s$=−1.5 eV. Black circles indicate the 555-777 defects.

is triggered by the diffusion of the single carbon atom 1 via the formation of bond with atom 6 as an intermediate state and with the corporation from atom 5 as shown in Figs. 4(b)–4(e). In Fig. 4(b), the carbon atom 1 breaks the bond with atom 4 and forms a bond with atom 6. In Fig. 4(c), the carbon atom 5 breaks bonds with atoms 7 and 8 and forms a bond with atom 1 to assist its diffusion. Then the carbon atom 1 breaks the bond with atom 3 in Fig. 4(d) and forms a bond with atom 7 in Fig. 4(e). In Fig. 4(f), the diffusion of 5-8-5 defect is completed via the diffusion of carbon atom 1. The 5-8-5 defect in Fig. 4(f) rotates clockwise by ~60° as compared to that in Fig. 4(a). The energy barrier for the "single atom diffusion" mechanism is found to be 6.9 eV by first principles LDA calculation.

We have also performed first-principles LDA calculation for a graphene layer containing four neighboring 555-777 defects to study the simulated STM image of the local haeckelite structure based on the theory of Tersoff and Hamann.[24] Atomic structures in Fig. 5(a) show the local haeckelite structure composed by four neighboring 555-777 defects. Figure 5(b) shows the corresponding simulated STM image of filled state at $V_s$=−1.5 eV. The simulated STM image shows salient topographic protrusions at the location of the pentagons. The result is very similar to the simulated STM image of carbon haeckelite structure where bright spots appear at the locations of pentagon pairs.[25] Our simulated STM image should be very useful for searching the local haeck-

elite structure in a graphite or carbon nanotube after the irradiation.

## IV. SUMMARY

We have performed TBMD simulation for a graphene layer with four scattered single vacancies. In the simulation, the single vacancies first coalesce into double vacancies of 5-8-5 defect structure and then further reconstruct into a local haeckelite structure consisting of two neighboring 555-777 defects. During the reconstruction process, we also observed three interesting mechanisms for the diffusion of a 5-8-5 vacancy. These mechanisms are "dimer diffusion," "chain diffusion," and "single atom diffusion" mechanisms. The simulated STM image of local haeckelite structure shows that the carbon atoms in pentagonal rings contribute to the bright spots.

## ACKNOWLEDGMENTS

The authors would like to acknowledge the support from KISTI under the 7th Strategic Supercomputing Applications Support Program. The use of the computing system of the Supercomputing Center is also appreciated. This work is supported by the Korea Research Foundation Grant funded by the Korea Government (MOEHRD) (KRF-2005-041-D00406). This work was supported by the BK21 Program through the Ministry of Education, Korea. Ames Laboratory is operated for the U.S. Department of Energy by Iowa State University under Contract No. W-7405-Eng-82. This work was also supported by the Director for Energy Research, Office of Basic Energy Sciences including a grant of computer time at the National Energy Research Supercomputing Center (NERSC) in Berkeley.

[1] J. G. Kushmerick, K. F. Kelly, H. P. Rust, N. J. Halas, and P. S. Weiss, J. Phys. Chem. B **103**, 1619 (1999).
[2] J. R. Hahn and H. Kang, Phys. Rev. B **60**, 6007 (1999).
[3] Q. M. Zhang, H. K. Kim, and M. H. W. Chan, Phys. Rev. B **33**, 413 (1986).
[4] B. T. Kelly, *Physics of Graphite* (Applied Science, London, 1981).
[5] P. M. Ajayan, V. Ravikumar, and J. C. Charlier, Phys. Rev. Lett. **81**, 1437 (1998).
[6] M. Menon and D. Srivastava, Phys. Rev. Lett. **79**, 4453 (1997).
[7] A. V. Krasheninnikov, K. Nordlund, J. Keinonen, and F. Banhart, Phys. Rev. B **66**, 245403 (2002).
[8] M. Terrones, F. Banhart, N. Grobert, J.-C. Charlier, H. Terrones, and P. M. Ajayan, Phys. Rev. Lett. **89**, 075505 (2002).
[9] Z. Tang, M. Hasegawa, T. Shimamura, Y. Nagai, T. Chiba, Y. Kawazoe, M. Takenaka, E. Kuramoto, and T. Iwata, Phys. Rev. Lett. **82**, 2532 (1999).
[10] P. A. Thrower, Chem. Phys. Carbon **5**, 217 (1969).
[11] E. Kaxiras and K. C. Pandey, Phys. Rev. Lett. **61**, 2693 (1988).
[12] M. Hjort and S. Stafström, Phys. Rev. B **61**, 14089 (2000).
[13] A. A. El-Barbary, R. H. Telling, C. P. Ewels, M. I. Heggie, and P. R. Briddon, Phys. Rev. B **68**, 144107 (2003).
[14] S. L. Mielke, D. Troya, S. Zhang, J. Li, S. Xiao, R. Car, R. S. Ruoff, C. Schatz, and T. Belytschko, Chem. Phys. Lett. **390**, 413 (2004).
[15] Y. Ma, P. O. Lehtinen, A. S. Foster, and R. M. Nieminen, New J. Phys. **6**, 68 (2004).
[16] M. S. Tang, C. Z. Wang, C. T. Chan, and K. M. Ho, Phys. Rev. B **53**, 979 (1996).
[17] G. D. Lee, C. Z. Wang, E. Yoon, N. M. Hwang, D. Y. Kim, and K. M. Ho, Phys. Rev. Lett. **95**, 205501 (2005).
[18] http://cms.mpi.univie.ac.at/vasp/
[19] G. Kresse and J. Furthmúller, Phys. Rev. B **54**, 11169 (1996).
[20] G. Kresse and J. Furthmúller, Comput. Mater. Sci. **6**, 15 (1996).
[21] D. Vanderbilt, Phys. Rev. B **41**, 7892 (1990).
[22] A. J. Stone and D. J. Wales, Chem. Phys. Lett. **128**, 501 (1986).
[23] H. Terrones, M. Terrones, E. Hernández, N. Grobert, J. C. Charlier, and P. M. Ajayan, Phys. Rev. Lett. **84**, 1716 (2000).
[24] J. Tersoff and D. R. Hamann, Phys. Rev. B **31**, 805 (1985).
[25] Ph. Lambin, G. I. Márk, and L. P. Biró, Phys. Rev. B **67**, 205413 (2003).